

8-1-1999

# Charge dynamics in the half-metallic ferromagnet $\text{CrO}_2$

E. J. Singley

Christopher P. Weber

*Santa Clara University*, [cweber@scu.edu](mailto:cweber@scu.edu)

D. N. Basov

A. Barry

J. M. D. Coey

Follow this and additional works at: <https://scholarcommons.scu.edu/physics>

 Part of the [Condensed Matter Physics Commons](#)

## Recommended Citation

Singley, E. J., Weber, C. P., Basov, D. N., Barry, A., & Coey, J. M. D. (1999). Charge dynamics in the half-metallic ferromagnet  $\text{CrO}_2$ . *Physical Review B*, 60(6), 4126–4130. <https://doi.org/10.1103/PhysRevB.60.4126>

Copyright © 1999 American Physical Society. Reprinted with permission.

This Article is brought to you for free and open access by the College of Arts & Sciences at Scholar Commons. It has been accepted for inclusion in Physics by an authorized administrator of Scholar Commons. For more information, please contact [rsroggin@scu.edu](mailto:rsroggin@scu.edu).

## Charge dynamics in the half-metallic ferromagnet CrO<sub>2</sub>

E. J. Singley, C. P. Weber, and D. N. Basov

*Department of Physics, University of California—San Diego, La Jolla, California 92093-0319*

A. Barry

*Department of Physics, Trinity College, Dublin 2, Ireland*

J. M. D. Coey

*Department of Physics, University of California—San Diego, La Jolla, California 92093-0319  
and Department of Physics, Trinity College, Dublin 2, Ireland*

(Received 6 August 1998; revised manuscript received 19 January 1999)

Infrared spectroscopy is used to investigate the electronic structure and charge carrier relaxation in crystalline films of CrO<sub>2</sub> which is the simplest of all half-metallic ferromagnets. Chromium dioxide is a bad metal at room temperature but it has a remarkably low residual resistivity ( $<5 \mu\Omega \text{ cm}$ ) despite the small spectral weight associated with free carrier absorption. The infrared measurements show that low residual resistivity is due to the collapse of the scattering rate at  $\omega < 2000 \text{ cm}^{-1}$ . The blocking of the relaxation channels at low  $\omega$  and  $T$  can be attributed to the unique electronic structure of a half-metallic ferromagnet. In contrast to other ferromagnetic oxides, the intraband spectral weight is constant below the Curie temperature.

[S0163-1829(99)14929-4]

Chromium dioxide is one of few binary oxides that are ferromagnetic metals. Acicular powders have long been used in particulate media for magnetic recording, but key aspects of the electronic structure of CrO<sub>2</sub> remain unexplored. Its resistivity  $\rho_{dc}$  is unusual: the residual resistivity  $\rho_0$  can be as small  $5 \mu\Omega \text{ cm}$ , but above 80 K,  $\rho_{dc}$  becomes strongly temperature dependent and exceeds  $1000 \mu\Omega \text{ cm}$  above the Curie temperature  $T_C = 390 \text{ K}$ ,<sup>1,2</sup> a value which is beyond the Ioffe-Regel limit. Hence, CrO<sub>2</sub> may be classified as a “bad metal.”<sup>3,4</sup> Following the original paper by Schwarz,<sup>5</sup> numerous band structure calculations indicate that CrO<sub>2</sub> is a half-metallic ferromagnet with completely spin-polarized spin-up electrons at  $E_F$  and a wide gap in the spin-down density of states (DOS).<sup>4,6–10</sup> Recently a 90% spin polarization at  $E_F$  has been measured in CrO<sub>2</sub> using superconducting point contact spectroscopy.<sup>11</sup>

Here we investigate the electronic structure and charge dynamics in CrO<sub>2</sub> by means of reflectance spectroscopy carried out over the frequency range from 500 GHz to near ultraviolet. Our experiments reveal an interband contribution to the complex conductivity that is in accordance with a band structure entailing a high degree of spin polarization of the electronic states at  $E_F$ . A half-metallic density of states implies a temperature- and frequency-dependent intraband scattering rate. The strong suppression of the scattering rate that we observe as  $\omega, T \rightarrow 0$  is consistent with this notion of a (partial) gap in the electronic DOS. We have also analyzed the temperature dependence of the electronic spectral weight ( $N_{eff}$ ). In contrast to other ferromagnetic oxides, such as the manganites, we find no variation of  $N_{eff}$  with temperature.

We measured the near-normal incidence reflectance  $R(\omega)$  of crystalline films of CrO<sub>2</sub> grown on a TiO<sub>2</sub> [110] substrate.<sup>2</sup> Films with thickness  $>5 \mu\text{m}$  were found to be completely opaque throughout the experimental frequency range  $14\text{--}37\,000 \text{ cm}^{-1}$  ( $2\text{--}4600 \text{ meV}$ ). Films were coated

*in situ* with gold or aluminum in the optical cryostat and the spectrum of the metal-coated sample was used as a reference.<sup>12</sup> Experimental errors due to diffuse reflectance are minimized with this procedure, allowing reliable absolute values of  $R(\omega)$  to be obtained. The complex conductivity  $\sigma(\omega) = \sigma_1(\omega) + i\sigma_2(\omega)$  was obtained from  $R(\omega)$  using Kramers-Kronig analysis. The uncertainty of  $\sigma(\omega)$  spectra due to both low- and high-frequency extrapolations required for Kramers-Kronig analysis are negligible in the frequency range where the actual data exist.

Raw reflectance spectra  $R(\omega)$  measured at  $T = 10 \text{ K}$ ,  $150 \text{ K}$ , and  $300 \text{ K}$  are plotted in Fig. 1. Reflectance at all temperatures gradually decreases with increasing  $\omega$  up to a “plasma minimum” at  $\omega \approx 12\,000 \text{ cm}^{-1}$  in accordance with the room temperature data by Chase.<sup>13</sup> Our specimens show higher reflectance in the visible and near-ultraviolet ranges than the values reported earlier.<sup>14</sup> The far-infrared reflectance is strongly temperature dependent:  $R(\omega)$  increases at low  $T$  by as much as 7% between  $500 \text{ cm}^{-1}$  and  $1000 \text{ cm}^{-1}$ . The temperature dependence of  $R(\omega)$  is confined to relatively low frequencies and vanishes at  $\omega > 3000\text{--}4000 \text{ cm}^{-1}$ . The sharp peaks in the far-infrared part of the spectrum ( $357 \text{ cm}^{-1}$ ,  $474 \text{ cm}^{-1}$ , and  $573 \text{ cm}^{-1}$ ) are due to optical phonons.

In Fig. 2 we plot the dissipative part of the optical conductivity  $\sigma_1(\omega)$  at 300 K. From this spectrum one can easily distinguish three major contributions to optical absorption: (i) coherent response of free carriers seen as a sharp peak at  $\omega \approx 0$ , (ii) a plateau in mid- and near-infrared ( $1000\text{--}8000 \text{ cm}^{-1}$ ) where the conductivity is nearly frequency independent, and (iii) the region of interband absorption with an onset at  $\omega \approx 12\,000 \text{ cm}^{-1}$ . The plateau seen in mid-infrared frequencies is not observed in the response of conventional metals. This featureless absorption is commonly found in conducting oxides<sup>15</sup> and is usually attributed to strong interaction of the carriers with magnetic excitations. The most

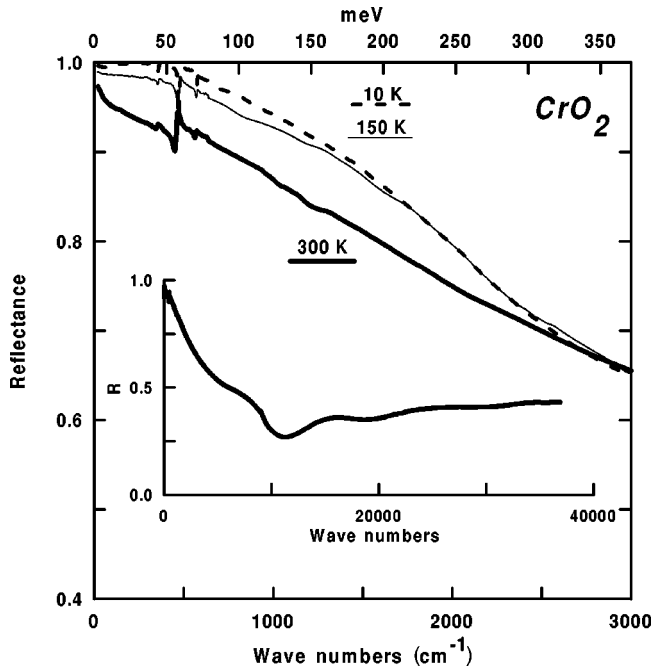


FIG. 1. Reflectance of  $\text{CrO}_2$  at 10 K, 150 K, and 300 K. Far-infrared reflectance is strongly temperature dependent and increases by as much as 7% at  $500 \text{ cm}^{-1}$ . The inset shows the 300 K reflectance over a broader energy scale.

appropriate analysis in this case is in terms of a single-component model where features (i) and (ii) are attributed to a single channel centered at zero frequency with a frequency-dependent effective mass  $m^*(\omega)$  and scattering rate  $1/\tau(\omega)$ .<sup>16,17</sup> However, close inspection of the conductivity spectra in Fig. 2 reveals the presence of a weak maximum at  $7000 \text{ cm}^{-1}$ , indicating a contribution of an interband transition. An attempt in separating the zero-frequency absorption channel from the mid-infrared absorption produced ambiguous results. In all likelihood the mid-infrared response is a combination of free carriers interacting with magnetic excitations and interband absorption. Due to the apparent weakness of the latter feature, we have chosen to present our analysis in terms of a single-component model. However, we will point out what effects the mid-infrared absorption will have on our results when relevant.

To understand the origin of the interband absorption (iii) it is instructive to define the effective spectral weight

$$N_{\text{eff}}(\Omega) = \frac{120}{\pi} \int_0^{\Omega} \sigma_1(\omega) d\omega. \quad (1)$$

$N_{\text{eff}}(\Omega)$  is proportional to the number of carriers participating in the optical absorption up to a certain cutoff frequency  $\Omega$ , and has the dimension of frequency squared. Integration of the conductivity up to  $\Omega = 12000 \text{ cm}^{-1}$ —the frequency at which we observe a clear onset of interband transitions—provides only 20% of the spectral weight we measure when  $\Omega$  is extended up to our experimental limit of  $37000 \text{ cm}^{-1}$ . This is actually an upper limit since an unknown portion of the integrated conductivity in the plateau region below  $12000 \text{ cm}^{-1}$  is due to intraband transitions, as discussed above. The relatively small amount of the spectral weight that can be attributed to coherent transport is consistent with

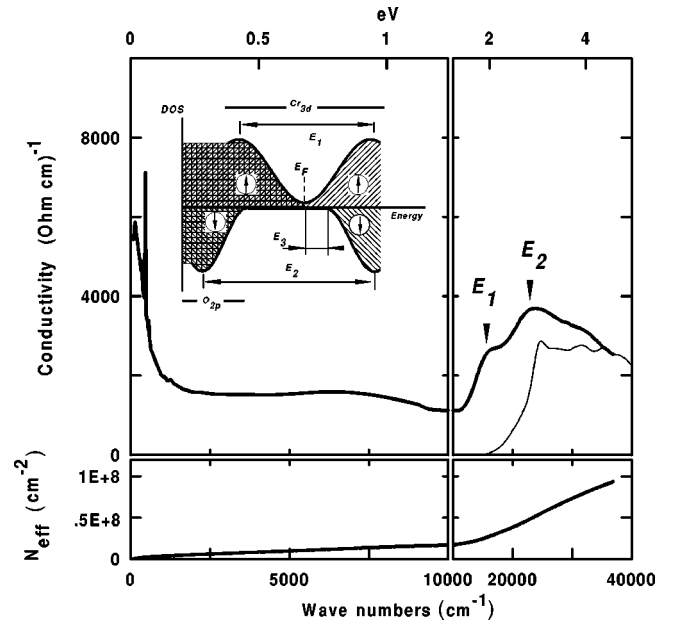


FIG. 2. Top panel: the frequency-dependent conductivity at 300 K. Arrows show the frequencies of the interband transitions:  $E_1 = 16000 \text{ cm}^{-1}$  and at  $E_2 = 27000 \text{ cm}^{-1}$ . The thin line shows the theoretical conductivity associated with the gap in the minority spin DOS (Ref. 8). Inset: schematic diagram showing the density of states in half-metallic  $\text{CrO}_2$  in the vicinity of the Fermi energy. Characteristic energies  $E_1 = 2.0 \text{ eV}$ ,  $E_2 = 3.35 \text{ eV}$ , and  $E_3 = 0.06\text{--}0.25 \text{ eV}$  are inferred from the infrared data as described in the text. Bottom panel: the effective spectral weight  $N_{\text{eff}}(\Omega)$  obtained from the integration of the conductivity as described in the text.

the notion that the Fermi energy in  $\text{CrO}_2$  is located in a *pseudogap* at the center of a band (derived from both oxygen  $p$  orbitals and chromium  $d_{yz}$  and  $d_{zx}$  orbitals) with a strongly depleted DOS (inset of Fig. 2). The reduced DOS near  $E_F$  is also seen in photoemission experiments which show a spectrum reminiscent of doped Mott-Hubbard insulators: most of the spectral weight is located in the upper and lower Hubbard bands but a clear metal-like edge is seen at  $E_F$ .<sup>18</sup> The first interband transition in the conductivity,  $E_1$ , is attributed to transitions across the pseudogap in the majority spin DOS. The position of the peak at  $16000 \text{ cm}^{-1} \approx 2 \text{ eV}$  is in excellent agreement with the photoemission results which find a separation of about 2 eV between peaks in the photoemission spectra. A similar pseudogap is suggested by band structure calculations.<sup>5,4,6–10</sup>

Another indication of the form of the DOS is provided by spin-polarized point contact spectroscopy measurements which find almost total spin polarization near  $E_F$ .<sup>11</sup> The nearly complete spin polarization implies a gap in the minority spin DOS. The resonance  $E_2$  at  $\omega = 27000 \text{ cm}^{-1} = 3.35 \text{ eV}$  is assigned to excitations across this gap. Uspenskii *et al.*<sup>8</sup> have used the local spin density approximation to calculate the optical conductivity of  $\text{CrO}_2$ . The result for the minority spin channel is shown as a thin line in Fig. 2. The calculated peak at 3.5 eV agrees very well with the location of the resonance  $E_2$ . Thus we conclude that the measured interband conductivity is in accordance with the half-metallic electronic structure of  $\text{CrO}_2$ .

The unique electronic structure of the half-metallic state also has a significant impact on the low-energy charge dy-

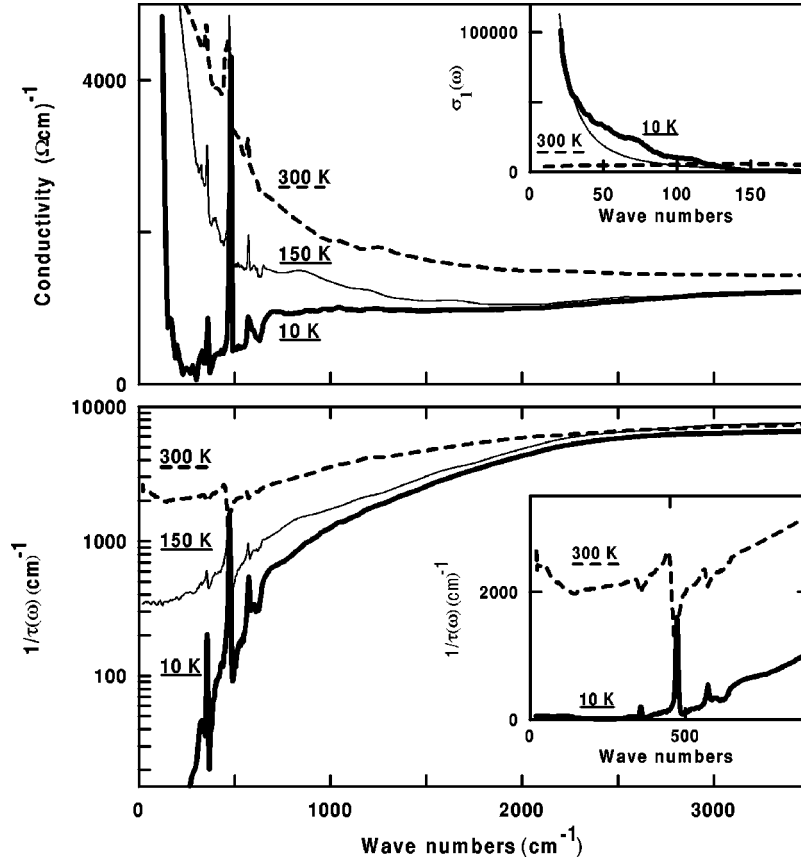


FIG. 3. Top panel: real part of the conductivity in far-infrared and mid-infrared frequencies at 300 K, 150 K, and 10 K. The conductivity narrows at low temperature so that the dc value is enhanced (a magnification of the far-infrared region is given in the inset). Thin line in the inset shows the Drude fit with the  $\rho = 5 \mu\Omega \text{ cm}$  determined with four-probe measurements and  $1/\tau^* = 13 \text{ cm}^{-1}$ . Bottom panel: spectra of the frequency-dependent scattering rate at 300 K, 150 K, and 10 K all show a threshold at  $\omega \approx 2000 \text{ cm}^{-1}$ . Inset: the dramatic suppression of  $1/\tau(\omega \rightarrow 0)$  at 10 K is illustrated.

namics. The low-frequency conductivity is shown in the top panel of Fig. 3. The conductivity is extremely temperature dependent. As the temperature is lowered the zero frequency peak narrows and the maximum increases, causing a rapid reduction of the dc resistivity at low  $T$ .<sup>2,19</sup> To clearly illustrate the magnitude of this effect the conductivity at 10 K and 300 K are replotted in the inset of the top panel of Fig. 3 on a different scale. The cause of the dramatic temperature dependence in the low-energy conductivity is most clearly understood in terms of the frequency-dependent scattering rate  $1/\tau(\omega)$ , which is a measure of the width of the zero-frequency peak at a given frequency. Following the single-component approach the spectra of  $1/\tau(\omega)$  can be obtained from the optical conductivity:

$$1/\tau(\omega) = \frac{\omega_{pD}^2}{4\pi} \text{Re} \left( \frac{1}{\sigma(\omega)} \right), \quad (2)$$

where the plasma frequency  $\omega_{pD} = 27000 \text{ cm}^{-1}$  was estimated from the integration of  $\sigma_1(\omega)$  up to the frequency of the onset of interband absorption at  $12000 \text{ cm}^{-1}$ . This value is to be taken as an upper limit due to the presence of the weak feature at  $7000 \text{ cm}^{-1}$ . The bottom panel of Fig. 3 shows a logarithmic plot of  $1/\tau(\omega)$  on the same frequency scale as the conductivity. We note that the frequency dependence of  $1/\tau(\omega)$  is confined to energies  $< 2000 \text{ cm}^{-1}$ . In this energy range the scattering rate is strongly suppressed as

the temperature is reduced. The inset in the bottom panel of Fig. 3 shows that in the limit  $\omega \rightarrow 0$  the scattering rate drops by two orders of magnitude between 300 K and 10 K.<sup>20</sup> This behavior of  $1/\tau$  reflected in the radical narrowing of the zero-frequency peak turns this “bad metal” at room temperature into an excellent conductor at low temperatures. The collapse of the scattering rate at low temperatures is consistent with recent magnetoresistance measurements on films of  $\text{CrO}_2$ .<sup>21,22</sup>

It can be argued that the evolution of the  $1/\tau(\omega)$  spectra with temperature is a natural consequence of the half-metallic DOS. Indeed the DOS sketched in the inset of Fig. 2 implies that at  $T=0$  spin-flip processes are forbidden for  $\omega$  below the energy  $E_3$  separating  $E_F$  from the bottom of spin-down band. This is because the final states of spin-down orientation required for spin-flip scattering are absent in this energy interval. Thus, half-metallic electronic structure precludes spin-flip scattering which is the dominant scattering mechanism in ferromagnets.<sup>23,24</sup> This can lead to a particularly strong effect in  $\text{CrO}_2$  because the magnetic scattering will be especially effective in this material, where there is an on-site Hund’s rule coupling of the  $d_{yz}, d_{zx}$  conduction electron and the  $d_{xy}$  core spin. At low temperature spin-flip relaxation channels, including scattering on magnons or magnetic impurities such as  $\text{Cr}^{3+}$ , are completely prohibited for  $\omega < E_3$ . Nonmagnetic scattering can also be reduced analo-

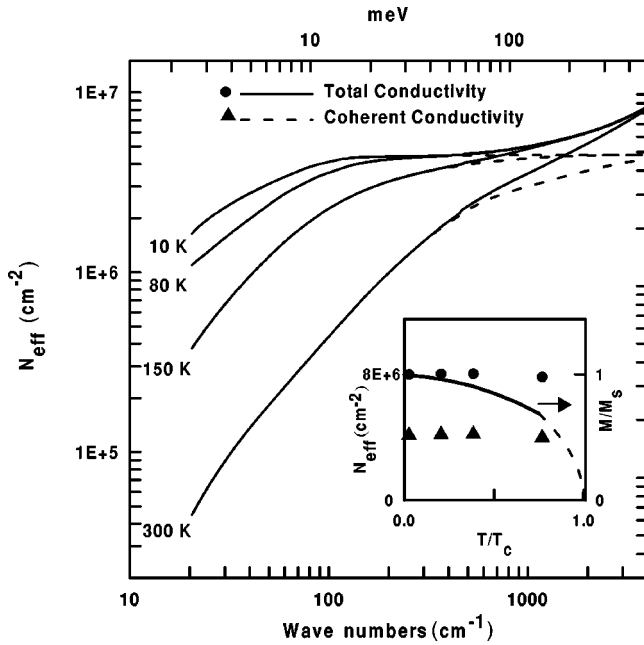


FIG. 4.  $N_{eff}$  from Eq. (1) plotted at 10 K, 80 K, 150 K, and 300 K. Solid lines represent integration of the total conductivity, while the dashed lines are only an integration of the coherent part of the conductivity (see Ref. 26). Inset:  $N_{eff}(\Omega = 4000 \text{ cm}^{-1})$  as a function of temperature. Solid circles are the total conductivity, while triangles are only the coherent part of the conductivity. The solid line is the magnetization normalized to its saturation value. The dashed line is the mean field theory extrapolation to  $T_c$ .

gous to the situation in high- $T_c$  superconductors in the regime where the normal-state pseudogap is opened.<sup>25,16</sup> At high temperature or high energy ( $\omega > E_3$ ) the spin-flip events are no longer forbidden and the scattering rate increases. From the spectra of  $1/\tau(\omega)$  we estimate the value of  $E_3$  to be between 500 and 2000  $\text{cm}^{-1}$  (60→250 meV).

While the relaxation rate of the conducting carriers is strongly temperature dependent, the intraband spectral weight is nearly constant. We emphasize that any variations of  $N_{eff}(\Omega)$  with temperature is confined to a frequency region comparable to  $1/\tau$ . In Fig. 4  $N_{eff}(\Omega)$  is plotted for several different temperatures. The solid lines represent the integration of both the coherent (i) and mid-infrared plateau (ii) parts of the conductivity. At low temperatures the spec-

tral weight is primarily acquired from the far-infrared frequency range. As the temperature increases the broadening of the zero-frequency peak causes the spectral weight to be spread throughout the mid-infrared frequency range. Above 4000  $\text{cm}^{-1}$ ,  $N_{eff}(\Omega)$  is temperature independent. Referring back to Fig. 2 we see that this limit is well below the onset of interband transitions. Thus, we find that the intraband spectral weight is constant at all temperatures. The inset of Fig. 4 shows  $N_{eff}(\Omega = 4000 \text{ cm}^{-1})$  as a function of temperature (solid circles). This analysis has also been applied to just the coherent part of the conductivity (Fig. 4, dashed lines).<sup>26</sup> Again we see that  $N_{eff}(\Omega = 4000 \text{ cm}^{-1})$  is independent of temperature (triangles in inset of Fig. 4).

Recently it has been suggested that  $\text{CrO}_2$  may be a self-doped double-exchange ferromagnet.<sup>9</sup> In other systems with double-exchange coupling a strong correlation exists between the magnetization and intraband spectral weight.<sup>27</sup> In the inset of Fig. 4 we also plot the temperature-dependent magnetization of  $\text{CrO}_2$  normalized to its saturation value. While the magnetization changes significantly over the measured temperature range,  $N_{eff}$  is constant. In contrast to the behavior seen in other double-exchange ferromagnets, the increased ordering of local moments seems to have little effect on the magnitude of the free carrier spectral weight in  $\text{CrO}_2$ .

In conclusion, we found that the signatures of the electromagnetic response of  $\text{CrO}_2$  include (i) reduced spectral weight of free carrier absorption suggestive of greatly depleted electronic density of states at  $E_F$ , (ii) interband transitions at 2 eV and 3.35 eV, and (iii) suppression of the scattering rate at low  $T$  and  $\omega$ . These effects involving high-energy interband absorption on the one hand and low-energy charge dynamics on the other can be understood in terms of the half-metallic nature of  $\text{CrO}_2$ . In contrast to other ferromagnetic oxides showing strong spin polarization, the effective free carrier spectral weight is independent of the magnetization.

The authors would like to thank P. B. Allen, A. Bratkovski, J. E. Hirsch, and I. I. Mazin for many useful comments. This work was supported by the NSF Grant No. DMR-9875980, the Alfred P. Sloan Foundation, a subcontract from Brookhaven National Laboratory, and a grant from Research Corporation. D.N.B. received funding from the Research Corporation.

<sup>1</sup>D.S. Redbell, J.M. Lommel, and R.C. DeVires, J. Phys. Soc. Jpn. **21**, 2430 (1966).

<sup>2</sup>L. Ranno, A. Barry, and J.M.D. Coey, J. Appl. Phys. **81**, 5774 (1997).

<sup>3</sup>V.J. Emery and S.A. Kivelson, Phys. Rev. Lett. **74**, 3253 (1995).

<sup>4</sup>S.P. Lewis, P.B. Allen, and T. Sasaki, Phys. Rev. B **55**, 10 253 (1997).

<sup>5</sup>K. Schwarz, J. Phys. F **16**, L211 (1986).

<sup>6</sup>E. Kulatov and I. Mazin, J. Phys.: Condens. Matter **2**, 343 (1990).

<sup>7</sup>H. van Leuken and R.A. de Groot, Phys. Rev. B **51**, 7176 (1995).

<sup>8</sup>Y.A. Uspenskii, E.T. Kulatov, and S.V. Halilov, Phys. Rev. B **54**, 474 (1996).

<sup>9</sup>M.A. Korotin, V.I. Anisimov, D.I. Khomskii, and G.A. Sawatzky,

Phys. Rev. Lett. **80**, 4305 (1998).

<sup>10</sup>I.I. Mazin, D.J. Singh, and C. Ambrosch-Draxl, Phys. Rev. B **59**, 411 (1999).

<sup>11</sup>R.J. Soulen, Jr., J.M. Byers, M.S. Osofsky, B. Nadgorny, T. Ambrose, S.F. Cheng, P.R. Broussard, C.T. Tanaka, J. Nowak, J.S. Moodera, A. Barry, and J.M.D. Coey, Science **282**, 85 (1998).

<sup>12</sup>C.C. Homes, M. Reedyk, D.A. Cradles, and T. Timusk, Appl. Opt. **32**, 2976 (1993).

<sup>13</sup>L.L. Chase, Phys. Rev. B **10**, 2226 (1974).

<sup>14</sup>We attribute this discrepancy to diffuse reflectance caused by rough surfaces of the samples studied earlier. Thin films investigated in this work had shiny surfaces and polishing was not required. Mechanical polishing was essential in Chase's mea-

surements but was not sufficient to produce a specularly reflecting surface; further correction for diffuse reflectance by as much as 12% was applied to the raw data. We emphasize that not only was the surface flatness superior in our experiments, but also the possible impact of minor roughness was accounted for by using the spectra of an *in situ* metal-coated sample as a reference.

- <sup>15</sup>For a review see: A. Georges, G. Kotliar, W. Krauth, and M. Rozenberg, *Rev. Mod. Phys.* **68**, 13 (1996); E. Dagotto, *ibid.* **66**, 763 (1994).
- <sup>16</sup>A.V. Puchkov, D.N. Basov, and T. Timusk, *J. Phys.: Condens. Matter* **8**, 10 049 (1996).
- <sup>17</sup>B.P. Stojkovic and D. Pines, *Phys. Rev. B* **56**, 11 931 (1997).
- <sup>18</sup>T. Tsujioka, T. Mizokawa, J. Okamoto, A. Fujimori, M. Nohara, H. Takagi, K. Yamaura, and M. Takano, *Phys. Rev. B* **56**, 15 509 (1997).
- <sup>19</sup>A. Barry, J.M.D. Coey, L. Ranno, and K. Ounadjela, *J. Appl. Phys.* **83**, 7166 (1998).
- <sup>20</sup>At 10 K the absolute value of the scattering rate  $1/\tau(\omega)$  is approaching the level of the noise ( $\sim 10 \text{ cm}^{-1}$  for  $\omega < 200 \text{ cm}^{-1}$ ). In a logarithmic plot such as Fig. 3 this noise will be greatly amplified. Therefore we stop the logarithmic plot at  $15 \text{ cm}^{-1}$  and show the complete low-energy portion of  $1/\tau(\omega)$  on a linear scale in the inset. To confirm that such a low value of the scattering rate is reasonable, we modeled the low-frequency conductivity at 10 K with a Drude formula  $\sigma(\omega) = \sigma_{dc} / [1$

$+ i\omega\tau^*]$ . (Inset in top panel, Fig. 3.) The value of  $1/\tau^* = 13 \text{ cm}^{-1}$  gave the best fit to the experimental data. This is consistent with our previously obtained value of  $20 \text{ cm}^{-1}$ .

- <sup>21</sup>K. Suzuki and P.M. Tedrow, *Phys. Rev. B* **58**, 11 597 (1998).
- <sup>22</sup>S.M. Watts, S. Wirth, S. von Molnar, A. Barry, and J.M.D. Coey (unpublished).
- <sup>23</sup>P.G. de Gennes and J. Friedel, *J. Phys. Chem. Solids* **4**, 71 (1958).
- <sup>24</sup>K. Kubo and N. Ohata, *J. Phys. Soc. Jpn.* **33**, 21 (1972).
- <sup>25</sup>D.N. Basov, R. Liang, D.A. Bonn, W.N. Hardy, and T. Timusk, *Phys. Rev. Lett.* **77**, 4090 (1996).
- <sup>26</sup>To ensure that the mid-infrared plateau was not masking any spectral weight transfer,  $N_{eff}(\Omega)$  was calculated again with this portion subtracted out. In the 10 K conductivity the coherent peak is clearly separated from the mid-infrared plateau at  $\omega = 300 \text{ cm}^{-1}$ . Everything below  $300 \text{ cm}^{-1}$  is attributed to the coherent response while the conductivity above  $300 \text{ cm}^{-1}$  is what we call the mid-infrared plateau. The coherent response at other temperatures is obtained by subtracting the 10 K mid-infrared plateau from the total conductivity at that temperature. The dashed lines in Fig. 4 represent the integration of these coherent conductivity spectra.
- <sup>27</sup>K.H. Kim, J.H. Jung, D.J. Eom, T.W. Noh, Jaejun Yu, and E.J. Choi, *Phys. Rev. Lett.* **81**, 4983 (1998).